

Article

Seismic Performance Assessments of RC Frame Structures Strengthened by External Precast Wall Panel

Seung-Ho Choi ¹, Jin-Ha Hwang ¹, Sun-Jin Han ¹, Hyo-Eun Joo ¹, Hyun-Do Yun ² and Kang Su Kim ^{1,*}

¹ Department of Architectural Engineering, University of Seoul, 163 Seoulsiripdae-Ro, Dongdaemun-Gu, Seoul 02504, Korea; ssarmilmil@gmail.com (S.-H.C.); jinhawang@gmail.com (J.-H.H.); sjhan1219@gmail.com (S.-J.H.); yoy8766@naver.com (H.-E.J.)

² Department of Architectural Engineering, Chungnam National University, 99 Daehak-Ro, Yuseong-Gu, Daejeon 34134, Korea; wiseroad@cnu.ac.kr

* Correspondence: kangkim@uos.ac.kr; Tel.: +82-2-6490-2762; Fax: +82-2-6490-5509

Received: 16 January 2020; Accepted: 2 March 2020; Published: 4 March 2020



Abstract: In recent years, a variety of strengthening methods have been developed to improve the seismic performance of reinforced concrete (RC) frame structures with non-seismic details. In this regard, this study proposes a new type of seismic strengthening method that compresses prefabricated precast concrete (PC) walls from the outside of a building. In order to verify the proposed method, a RC frame structure strengthened with precast walls was fabricated, and cyclic loading tests were performed. The results showed that specimens strengthened using the proposed method exhibited further improvements in strength, stiffness and energy dissipation capacity, compared to RC frame structures with non-seismic details. In addition, a nonlinear analysis method, capable of considering the flexural compression and shear behaviors of the walls, was suggested to analytically evaluate the structural behavior of the frame structures strengthened by the proposed method. Using this, an analysis model for frame structures strengthened with precast walls was proposed. Through the proposed model, the analysis and test results were compared in relation to stiffness, strength, and energy dissipation capacity. Then, the failure mode of the column was evaluated based on the pushover analysis. In addition, this study proposed a simplified analysis model that considered the placement of longitudinal reinforcements in shear walls.

Keywords: seismic strengthening; cyclic behavior; precast wall; nonlinear analysis

1. Introduction

As a large number of RC frame structures with non-seismic details have been severely damaged, many researchers [1–6] have investigated the infill wall-strengthening method to improve seismic performance by inserting cast-in-place concrete or precast (PC) walls inside the beam–column frame structure. The infill wall-strengthening method has the advantages that it is cost effective, while greatly increasing shear strength. However, it is not easy to secure the sufficient shear resistance performance of the connection due to the complex connection details between the RC frame and the infill wall; moreover, during the construction period, the use of internal space is very limited. In order to overcome the shortcomings of the conventional infill wall-strengthening method, various strengthening methods have been proposed. Frosch [2] presented the shear key connection details of PC panels to improve the infill wall-strengthening method, and Almusallam and Al-Salloum [3] proposed a strengthening method using the fiber reinforce polymer (FRP). Ozden et al. [4] investigated a strengthening method using CFRP hollow clay tiles, and Baran and Tankut [5] suggested a PC panel-strengthening method

using epoxy mortars. This study proposes an advanced seismic strengthening method using the externally anchored precast wall panel (EPCW). The EPCW method proposed in this study can significantly shorten the construction period, because the precast wall panels are connected with the existing frames on the outside of the building. Furthermore, there is an advantage in that the internal space can be used, even during construction. In this study, the specimens of RC frame structures with non-seismic details that are strengthened by the EPCW method are subjected to cyclic loading tests, to verify the strengthening performance of the EPCW. In addition, an analysis method is proposed, and the accuracy of the proposed model is verified by comparing the analytical and test results.

2. Experimental Investigation

2.1. Test Specimens

In order to verify the seismic performance of RC frame structures strengthened with EPCWs, a total of four specimens were fabricated, using as variables the method of connection between the frame and the wall, and the size of the EPCW. In consideration of the laboratory conditions, the specimens were made of 1/3 scaled one-bay single-story frames. Specimen FC shown in Figure 1 is a non-strengthened RC frame specimen, and the cross sections of the columns and beams are 150×150 mm and 150×250 mm, respectively. Specimen FBC is a specimen in which the EPCW is connected to the beam and column, as shown in Figures 2 and 3, where Figure 2 shows the details of the anchoring. It should be noted that the PC walls were separately cast from the frame structures in the same way that they are cast for retrofitting in the field. The size of the EPCW is $1200 \times 1000 \times 70$ mm. For the Specimen FB, all the details are the same as Specimen FBC; however, the EPCW is connected only to beams, not to columns. Specimens FBC and FB are used to investigate differences in behavior, according to the connection location of the PC wall and the existing RC frame.

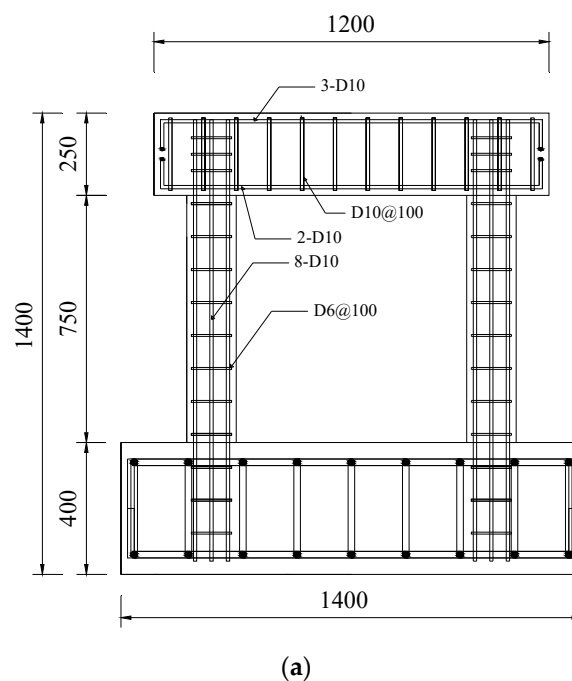
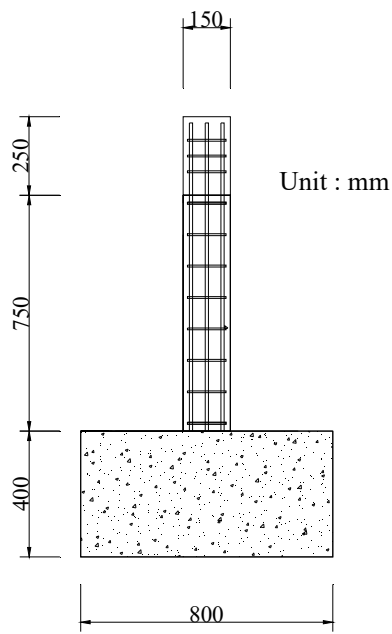


Figure 1. Cont.



(b)

Figure 1. Details of Specimen FC (unit: mm): (a) front view; (b) side view.

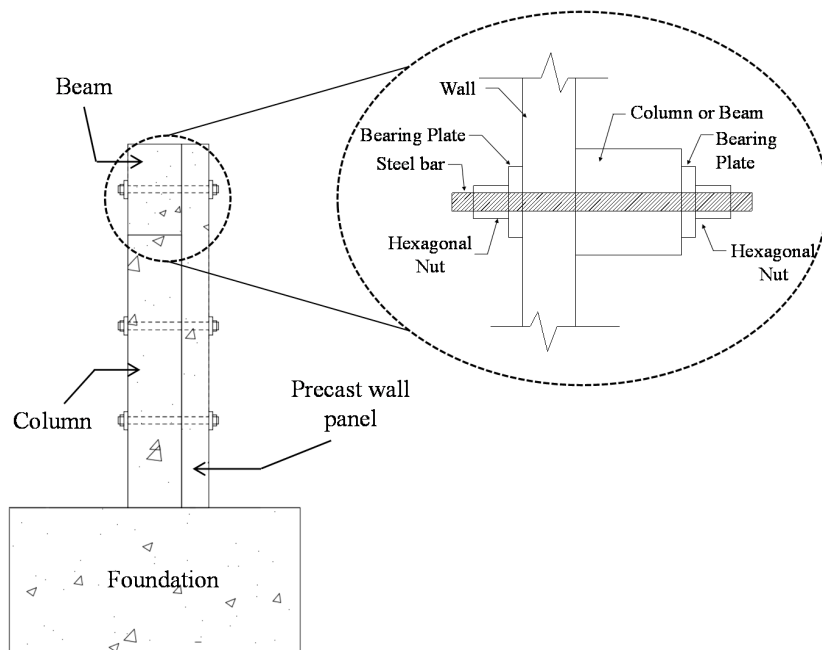


Figure 2. Details of externally anchored precast wall panel.

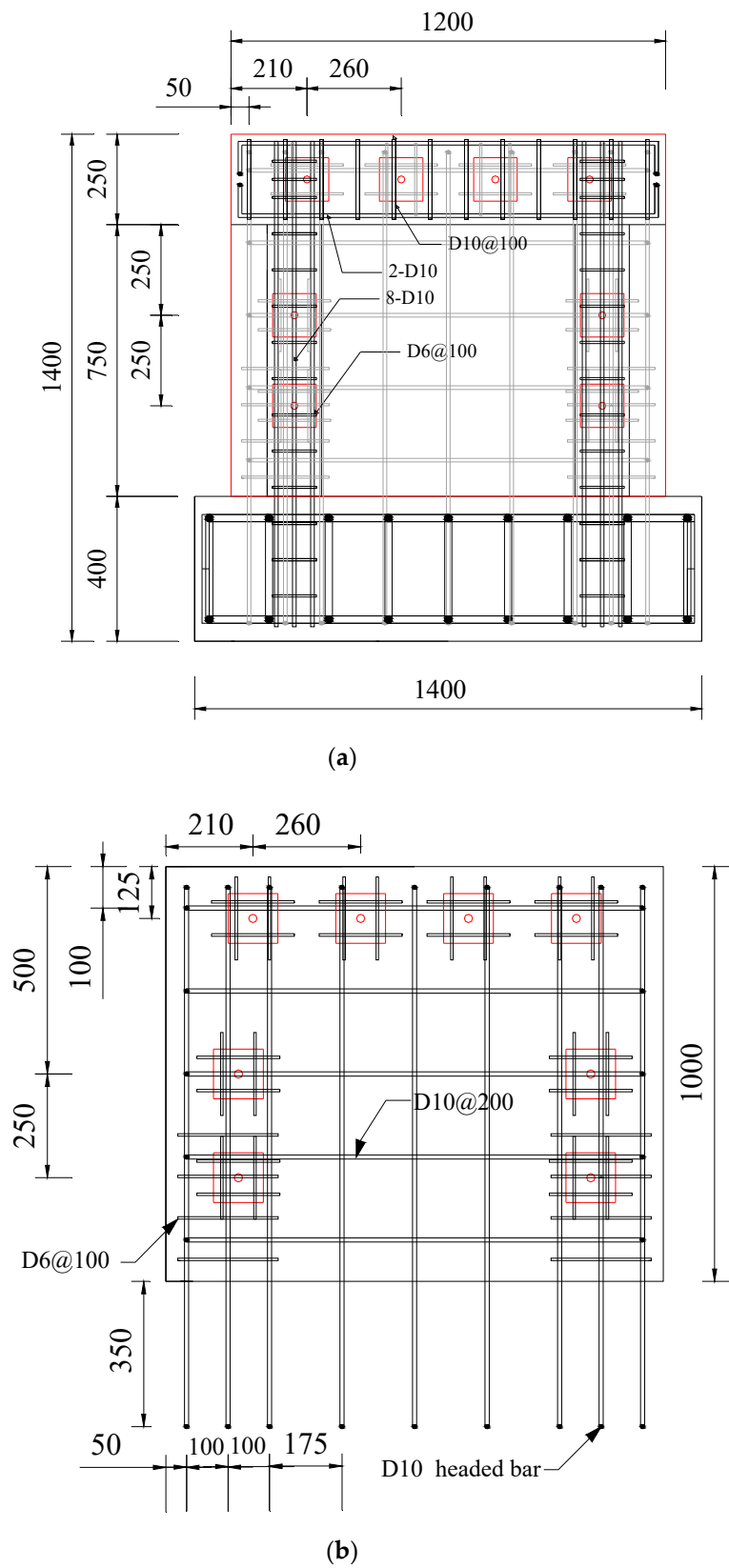


Figure 3. Details of Specimen FBC (unit: mm): (a) reinforcement details of frame; (b) reinforcement details of wall.

Specimen FPB, shown in Figure 4, is a specimen of two strengthened EPCWs either side of a column, in the form of a wing wall. The dimensions of each EPCW are $350 \times 1000 \times 70$ mm, which correspond to 1/4 of the EPCW applied to Specimens FBC and FB. The PC wall applied to Specimen FPB is designed to facilitate lifting operations and transportation by reducing its size. Moreover, it has excellent constructability. The PC walls were connected to the foundation using D10 headed bars, as shown Figures 3b and 4b. The EPCW and RC frame are connected using high-strength anchor bolts. The high-strength anchor bolts have a diameter of 26.5 mm, their yield and tensile strengths are 900 and 1100 MPa, respectively, and their elastic modulus is 205,000 MPa. The high-strength anchor bolts are assembled using hexagonal nuts and bearing plates, as shown in Figure 2. In addition, a strain gage is attached to the center of the anchor bolts to tighten the nuts until it they are about $300 \mu\epsilon$, so that the same tensile force is introduced to the anchor bolts. In the frame and EPCW, concrete with a compressive strength of 21.8 MPa is used. The yield and tensile strengths of the D6 reinforcement are 381 and 426 MPa, and those of the D10 reinforcement are 502 and 619 MPa, respectively.

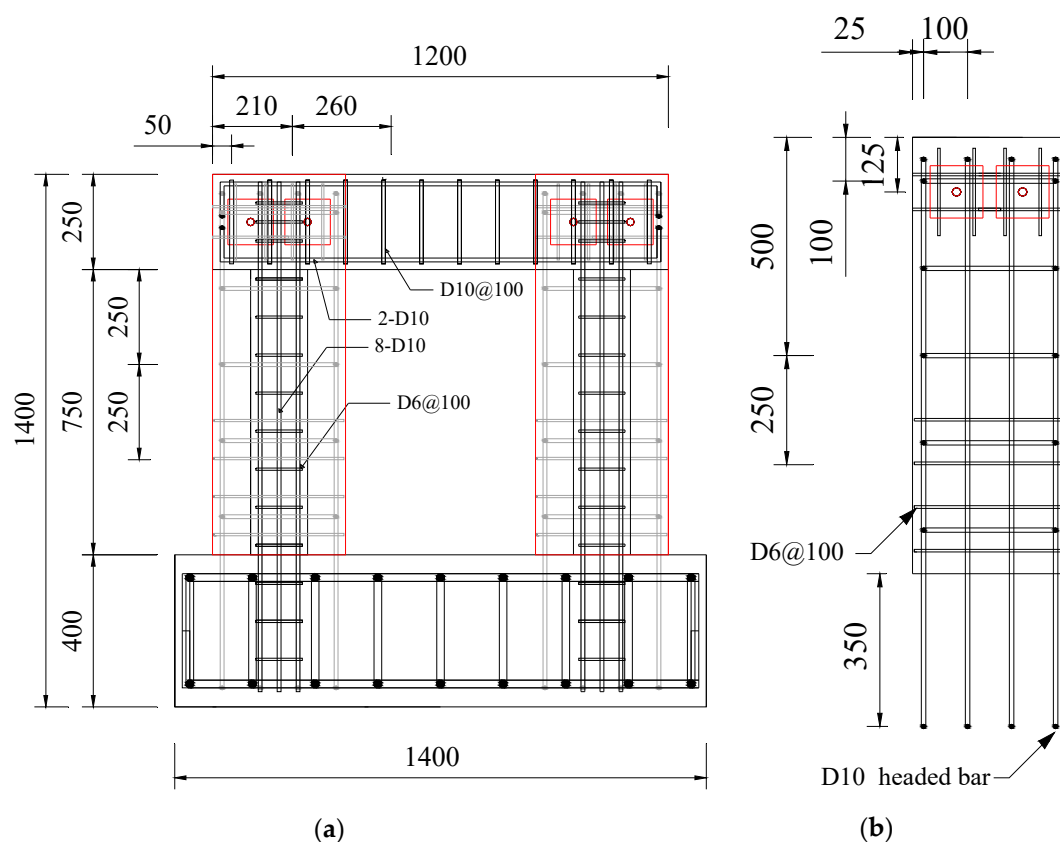


Figure 4. Details of Specimen FPB (unit: mm): (a) reinforcement details of frame; (b) reinforcement details of wall.

2.2. Test Procedure

Figure 5 shows the test specimen installed in a loading frame. For axial loads, 10% of the specimen's axial strength, including the axial strength of each wall, is kept constant under load control using a 1000 kN hydraulic actuator, until the end of the test. For lateral loads, displacement-controlled loading is applied using a 1000 kN capacity electric actuator. Figure 6 shows that iterative loading is applied three times at all story drift ratios in accordance with the preset target drift ratio (lateral displacement/height of the specimen).

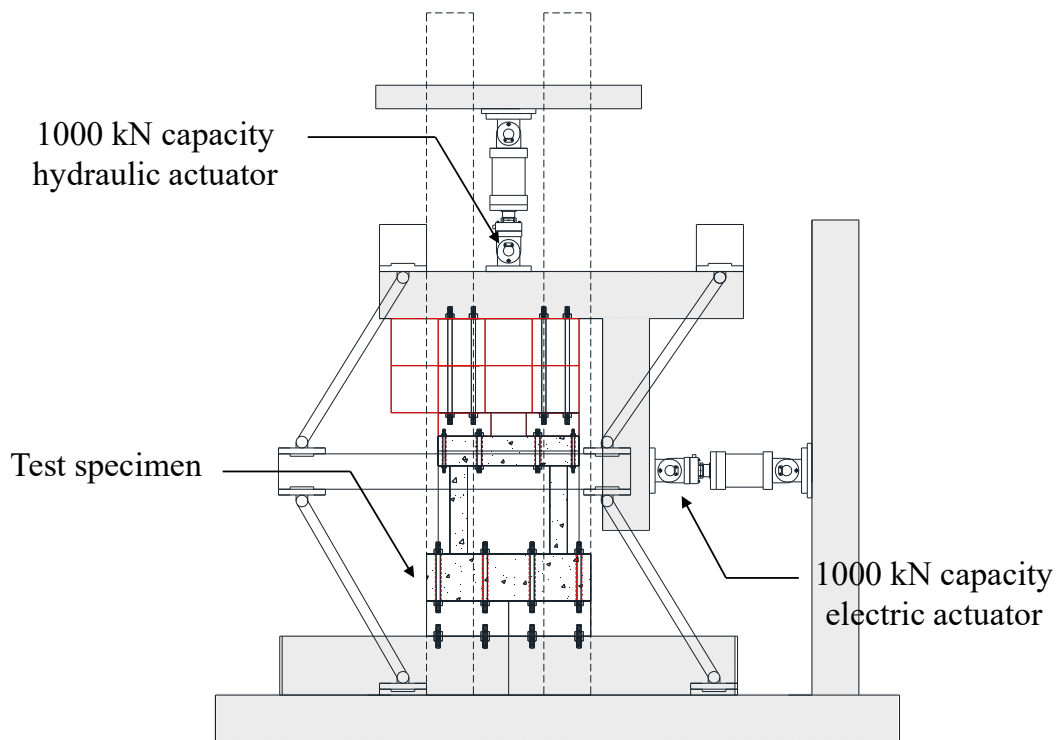


Figure 5. Test setup.

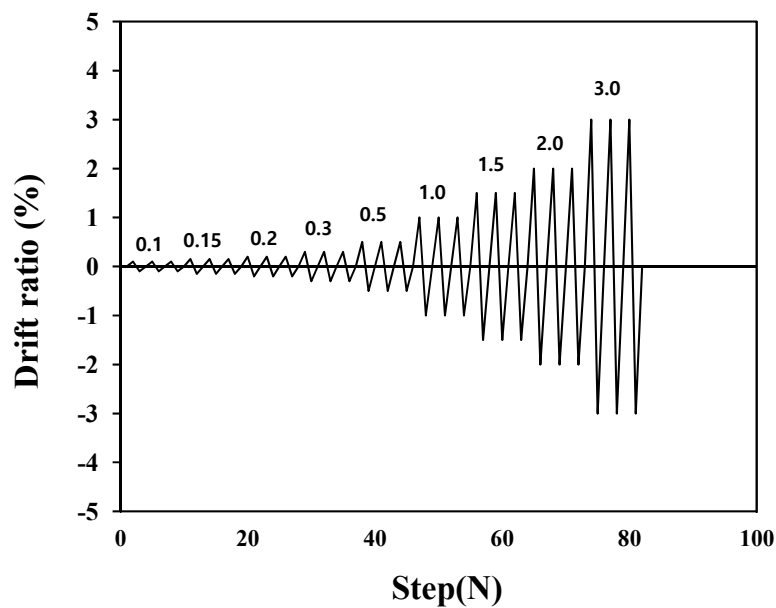


Figure 6. Loading steps.

3. Experimental Results

3.1. Behavior of Test Specimens

Figures 7 and 8 show the crack patterns and photographs of test specimens after failure. For Specimen FC, the strength was reduced to 78% of the maximum load, as the cover peeled off at the top of the column after the first load cycle at 2.0% drift ratio. The test was then terminated in accordance with laboratory safety regulations. Specimen FBC achieved 90% of the maximum load at 2.0% drift ratio, but underwent failure as the load rapidly decreased during loading in the negative

direction. This occurred after loading in the positive direction with a drift ratio of 2.0%. For Specimen FBC, as the EPCWs were connected to both the columns and the beam, significant crack damage was observed in the vicinity of the anchor bolts installed at the bottom of the columns, as shown in Figures 7b and 8b. Specimen FB, in which the EPCW was connected only to the beam, underwent separation between the frame and the EPCW as the concrete peeled off at the EPCW–foundation connections at a 2.0% drift ratio. In terms of Specimen FB, the crack widths observed from the columns were smaller, while those observed from the walls were larger, compared to those of Specimen FBC. For Specimen FB, the strength was reduced to 65% of the maximum load at the third cycle with a drift ratio of 2.0%, and the test was terminated after the loading of the third cycle. In Specimen FB, where the EPCW was connected only to the beam with anchor bolts, relatively small damage was observed in the columns, as shown in Figures 7c and 8c, compared to Specimen FBC. In Specimen FPB, to which two EPCWs were applied near the column in the form of wing walls, there was no significant decrease in the load, even at 2.0% drift ratio, and the test was terminated after loading at up to 3% drift in the positive direction. The load at 3.0% drift ratio was 94% of the maximum load, showing stable behavior without a significant decrease in load. Specimen FPB observed less damage in RC frames compared to other specimens, as shown in Figures 7d and 8d.

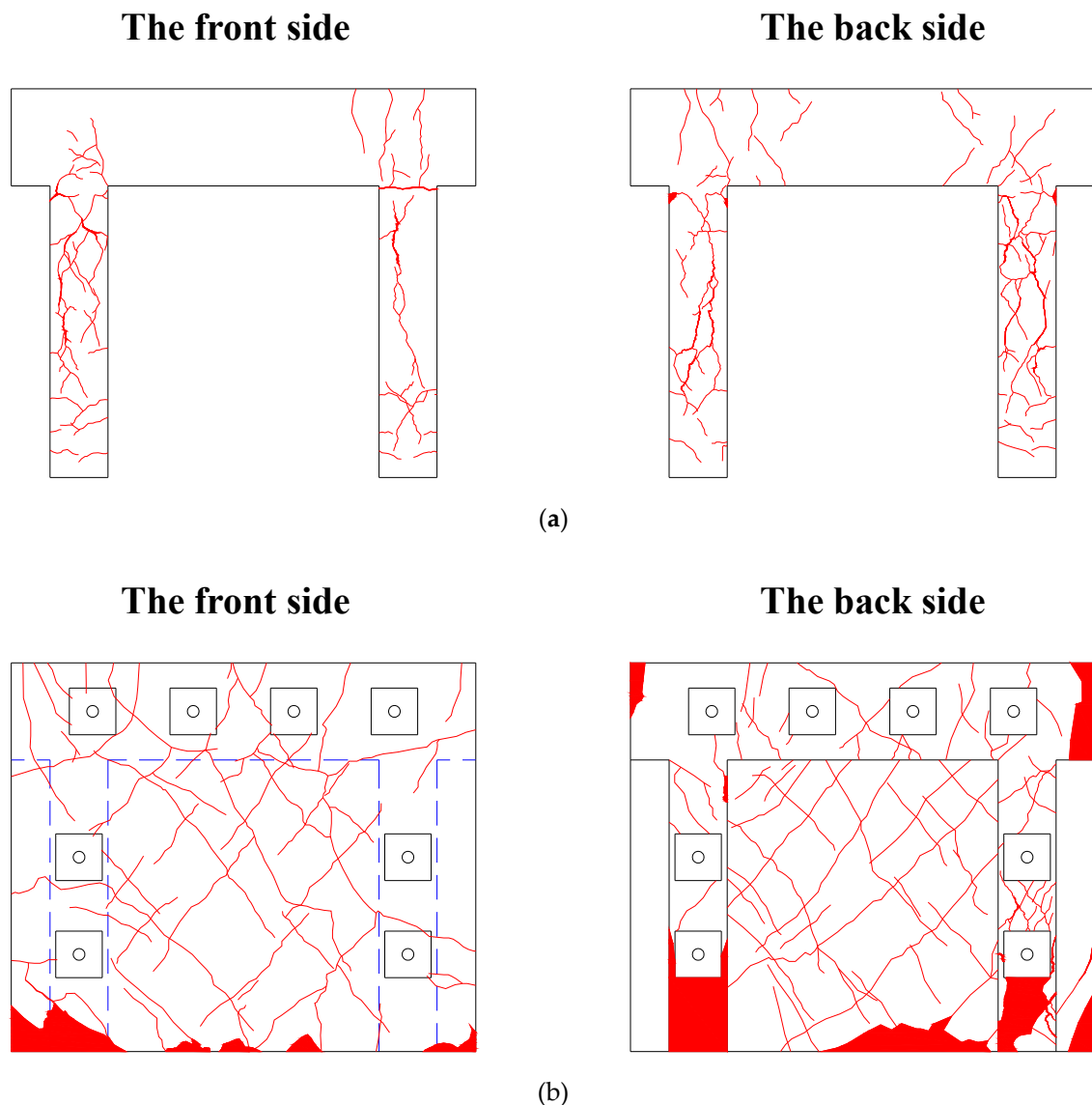


Figure 7. Cont.

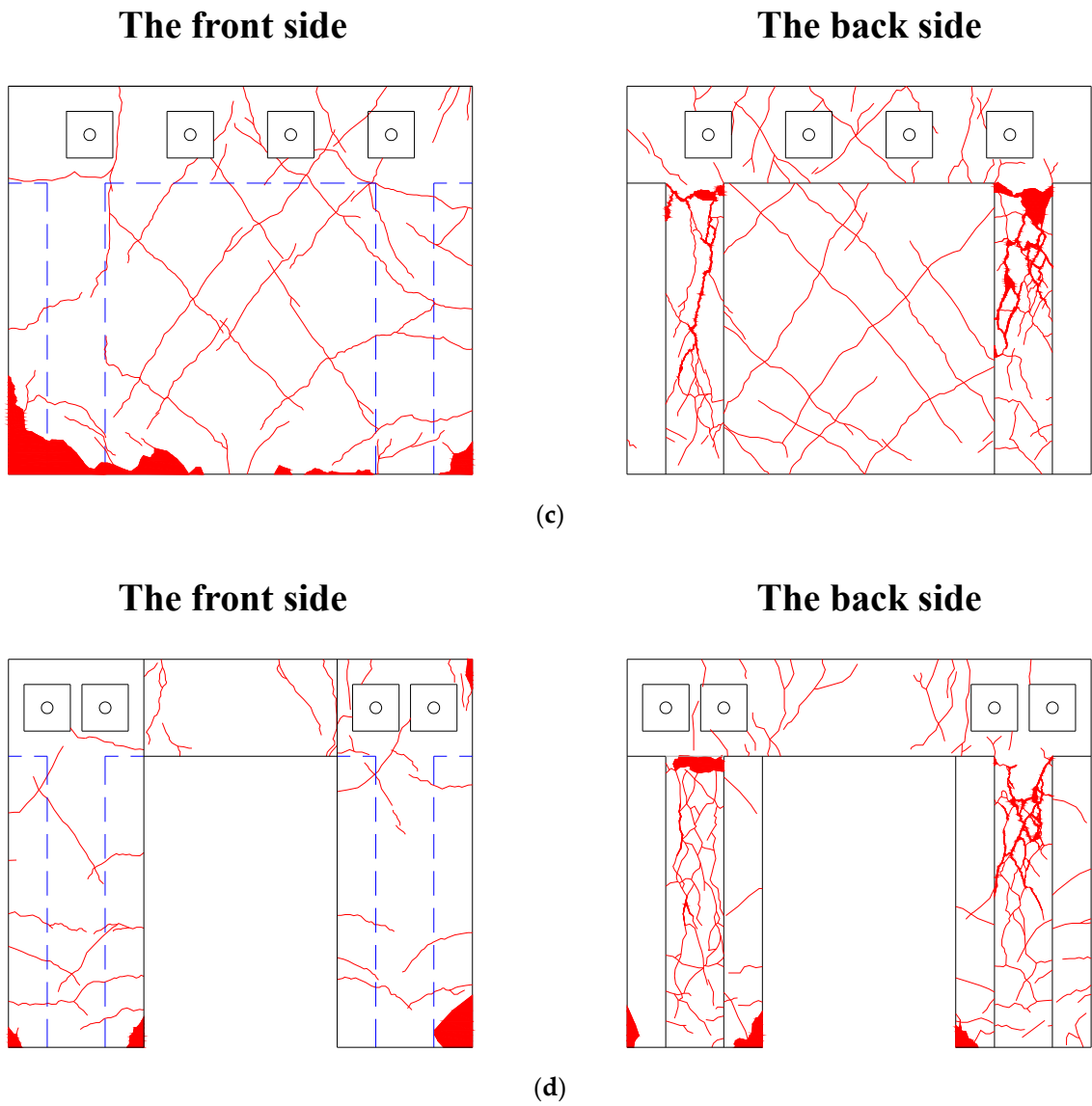


Figure 7. Observed crack patterns of specimens after failure: (a) Specimen FC; (b) Specimen FBC; (c) Specimen FB; (d) Specimen FPB.

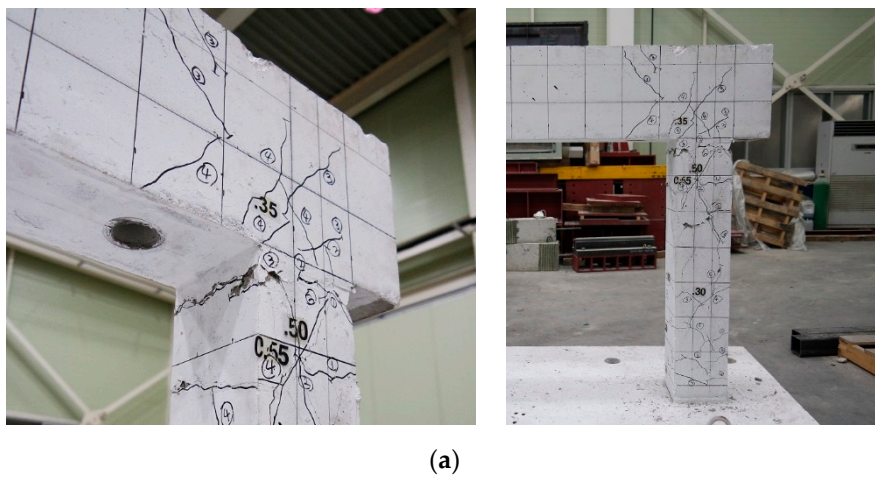


Figure 8. Cont.

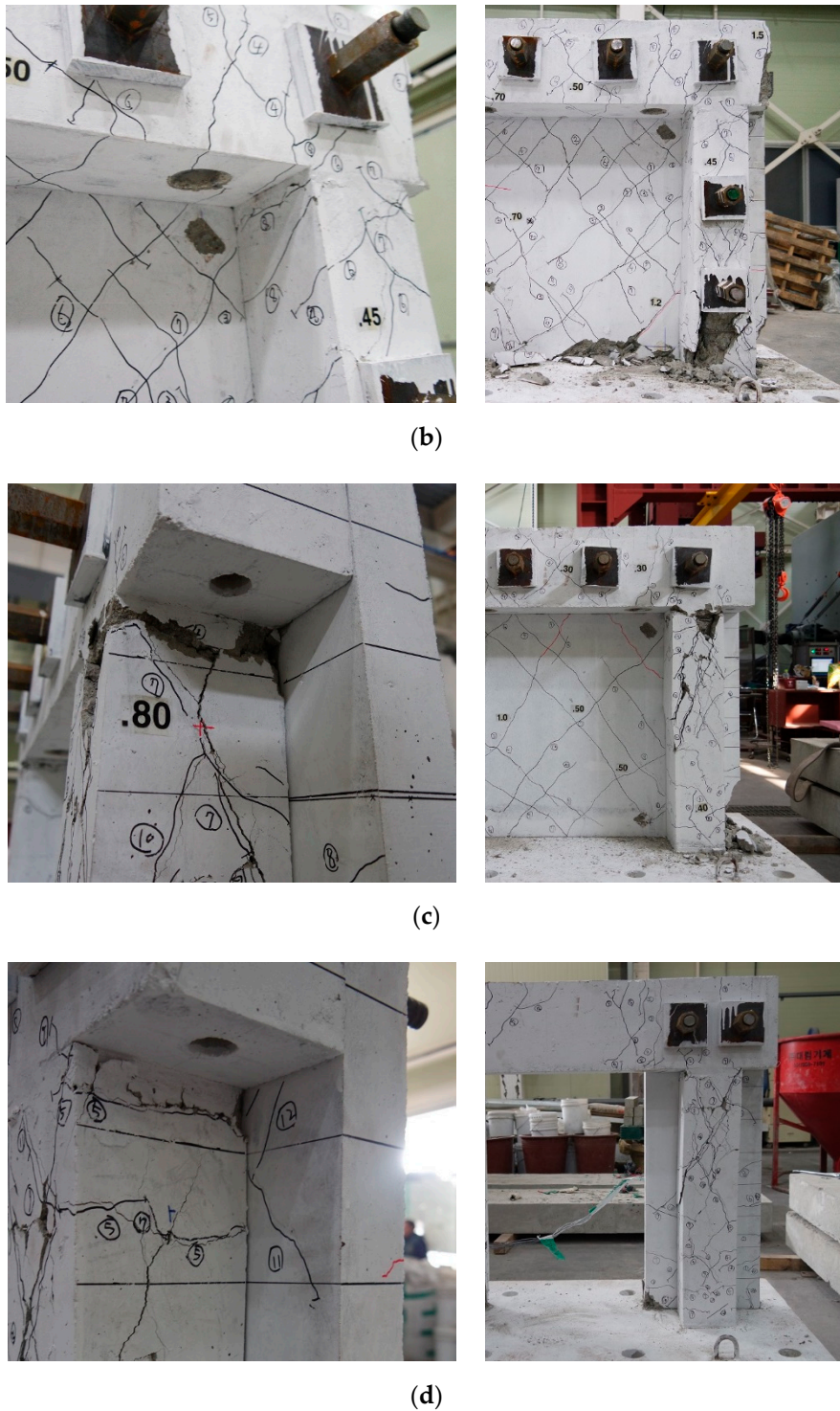


Figure 8. Photographs of specimens after failure: (a) Specimen FC; (b) Specimen FBC; (c) Specimen FB; (d) Specimen FPB.

When the conventional infill wall-strengthening method is used for the purpose of increasing the strength, the lateral stiffness and strength are greatly improved, but the lateral deformation capacity tends to significantly decrease. In addition, if the shear strength ratio of the infill wall to the existing RC frame is large, shear failure of the column may occur [7,8] which, when seismic strengthening is performed, is not a desirable failure mode. In the EPCW method proposed in this study, there was no reduction in lateral deformation capacity after strengthening, compared to the frame structures before

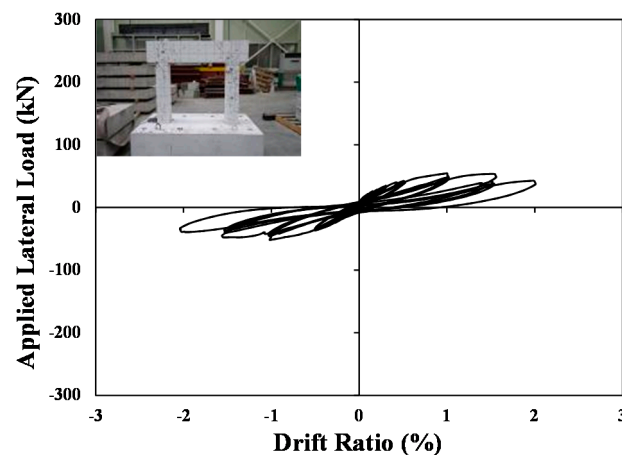
strengthening. In addition, in all specimens, the failure of the walls occurred prior to the shear failure of the column. These results suggest that efficient seismic strengthening has been achieved.

Figure 9 shows the load–displacement curves of Specimens FC, FBC, FB and FPB. The pinching effect was not significant in all specimens. Figure 9a shows that the maximum load of Specimen FC was 54.6 kN in the positive direction, and -51.7 kN in the negative direction. In both the positive and the negative directions, the maximum load occurred at 1.0% drift ratio, and there was then a gradual decrease in load. Figure 9b shows that the maximum load of Specimen FBC was 240.1 kN in the positive direction, and -272.1 kN in the negative direction. Specimen FBC showed a maximum load in the positive direction at 1.0% drift ratio, and a maximum load in the negative direction at 1.5% drift ratio. The maximum load of Specimen FBC was 4.4 and 5.26 times higher in the positive and negative directions, than that of Specimen FC. Figure 9c shows that Specimen FB showed its maximum load at 1.0% drift ratio. It was measured at 238.9 kN in the positive direction, and -216.9 kN in the negative direction. This suggests improvements in strength of 4.4 times in the positive direction, and 4.2 times in the negative direction, when compared to Specimen FC.

Although Specimens FBC and FB showed a slight difference in behavior in the negative direction, their overall behavior was similar. Figure 9d shows that in Specimen FPB, the maximum load occurred at 1.5% drift ratio, of 150.9 kN in the positive direction, and -158.1 kN in the negative direction. When compared to Specimen FC, the strength was improved 2.76 times in the positive direction, and 3.06 times in the negative direction.

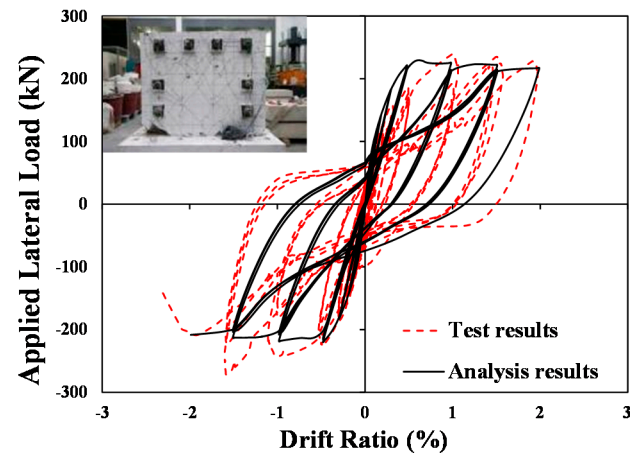
3.2. Behavior of Anchor Bolts

The strains of anchor bolts were measured during the test, and Figure 10 shows the lateral load–average strain relationship for the anchor bolts installed at the beam and column, respectively, for Specimen FBC. The bolt strains were found to be less than $200 \mu\epsilon$, which are the same for the other specimens. Although no instruments were installed to measure the slippage between the RC frame and the EPCW, no slippage was observed visually during the test.

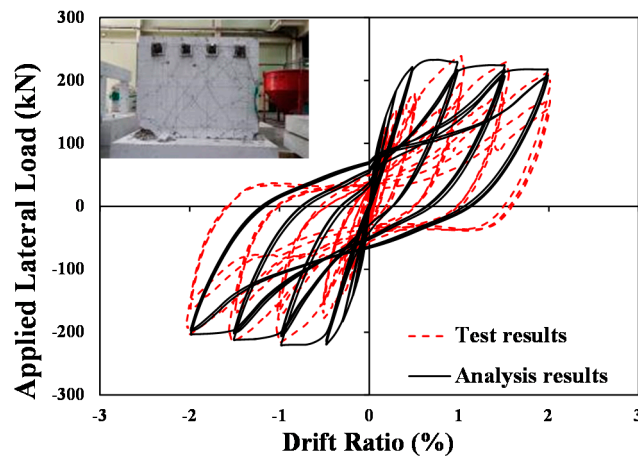


(a)

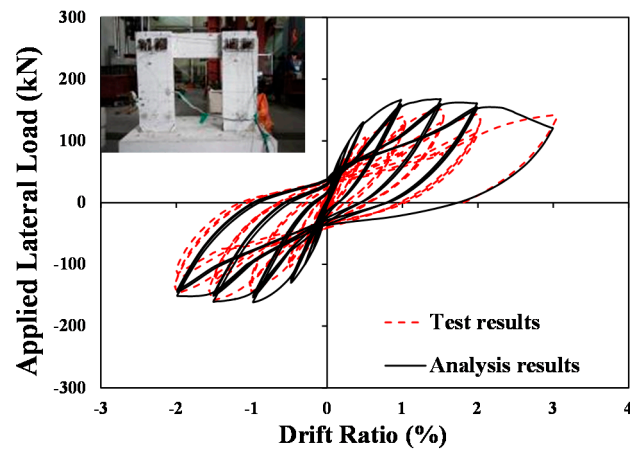
Figure 9. Cont.



(b)

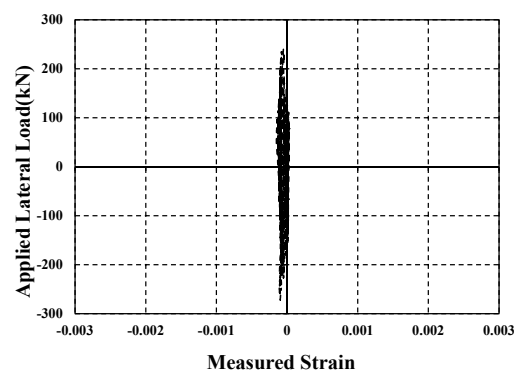


(c)

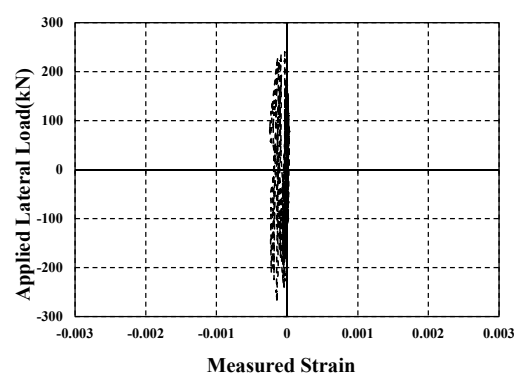


(d)

Figure 9. Lateral load-drift ratio of specimens: (a) Specimen FC; (b) Specimen FBC; (c) Specimen FB; (d) Specimen FPB.



(a)



(b)

Figure 10. Lateral load-strain relationship of anchor bolts: (a) at beam (Specimen FBC) (b) at column (Specimen FBC).

4. Analytical Approach

Many researchers [9–14] have developed nonlinear analysis methods to evaluate the behavior of reinforced concrete walls. In this study, the RC frame structures with non-seismic details were modeled as nonlinear beam–column elements [15–18], and the modeling of the walls was modified by applying the longitudinal and diagonal line element model (LDLEM) [14,19].

Figure 11a shows that the LDLEM consists of a beam element with infinite stiffness, and longitudinal and diagonal elements. It is a technique of modeling the longitudinal element to resist flexure, and the diagonal element to resist shear. In LDLEM, the diagonal member simulates the web concrete that resists shear force and is modeled to resist both tension and compression. Previous studies [10,11,20] have mainly dealt with barbell-type shear walls or infill wall analysis for seismic strengthening with the use of LDLEM. However, in this case, the two-dimensional elements can be modeled, because the frame and the wall are located on the same plane. For the PC wall proposed in this study, since the precast wall is attached and fixed by anchor bolts on the face the RC frame, it needs to be modeled as a three-dimensional element, unlike in the previous analysis. For this, the precast wall was modeled using LDLEM, and the RC frame was modeled to be in front of the wall as a fiber section.

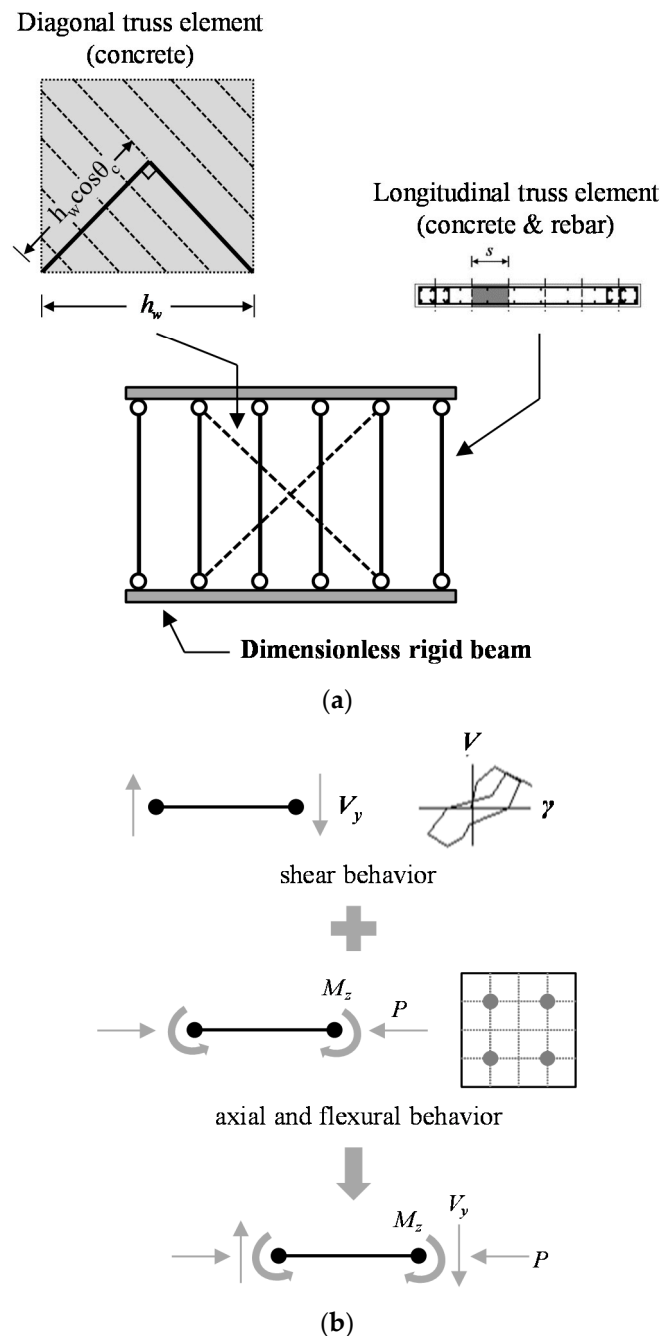


Figure 11. Analytical modeling approach: (a) longitudinal and diagonal line element model (LDLEM) modeling (Park and Eom, 2007); (b) Section aggregator.

In general frame structures, bending moment and shear force are generated simultaneously in a beam by seismic loads. However, in the fiber section model, only the behavior of axial force and the bending moment can be defined. In this study, a section aggregator (OPENSSES 2004) [21] was used to reflect the shear behavior in the analysis. The section aggregator analyzes the axial and flexural behaviors with the use of a general fiber section model, as shown in Figure 11b, and reflects the shear force–displacement response defined separately. In this study, the shear behavior of the RC columns was analyzed using a modified compression field theory (MCFT) [22,23], and the results were then reflected in the fiber section through the section aggregator.

The column concrete is modeled by dividing it into the confined concrete inside the lateral reinforcement, and the unconfined concrete outside. For the material model of concrete, Yassin (1994)'s

model [24] was used; while for the confined concrete, Mander (1988)'s model [25] was used. The reinforcement was modeled using the Giuffr -Menegotto-Pinto model [26]. As described above, for the shear behavior of the column member, the analysis result estimated using MCFT was modeled as the backbone curve of the Pinching 4 model [27] and added to the fiber section analysis model with the use of the section aggregator. With respect to the loading/unloading stiffness and strength degradation characteristics of the Pinching 4 model, the cyclic shear behavior was defined based on the test results of the column, as shown in Figure 12.

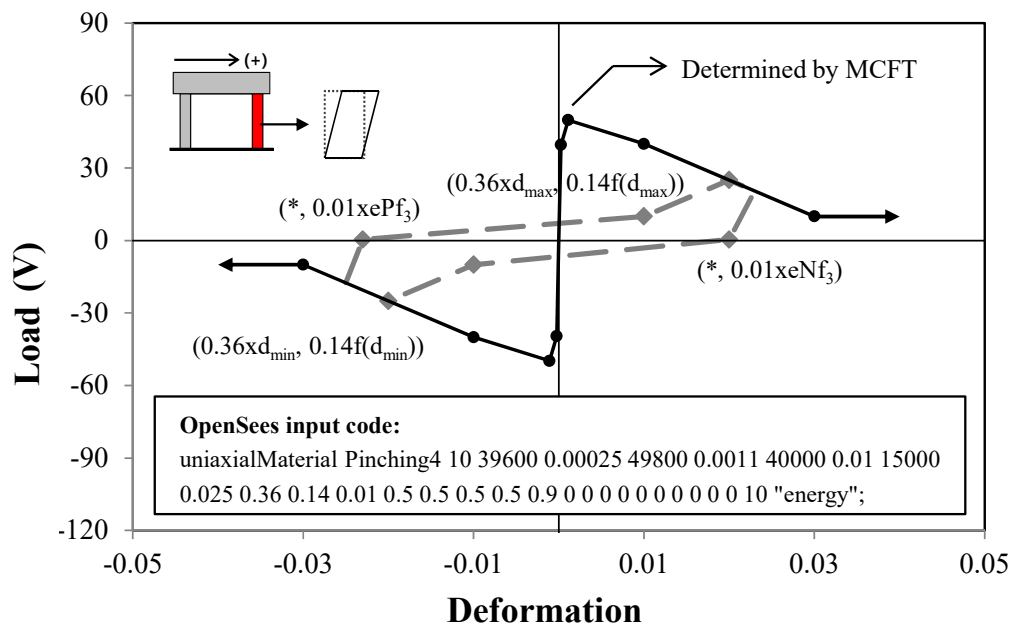


Figure 12. Hysteretic shear behavior of reinforced concrete column.

Figure 13 shows the finite element modeling details of Specimens FB, FBC and FPB, respectively. In the Specimen FB model presented in Figure 13a, 11 rebar and concrete elements were modeled to match the location of the longitudinal reinforcement placed on the specimen. The inclination angle of the diagonal element, corresponding to the compression strut of the wall, was modeled to 45 degrees to fit the squat wall. In existing shear wall analysis models [10,11,20], since the focus has been placed more on the behavior of the wall when modeling barbell-type shear walls or infill walls, the connection between the column and beam was modeled as a pinned connection in the same way as other longitudinal elements. However, when the RC frame is strengthened with EPCW, it is appropriate to model the beam-column connection as a fixed end, since the failure mode and behavior of the RC frame can affect the strengthened frame. Therefore, Figure 11 shows that in this study, the connection between the beam and column of the RC frame was set as the fixed end. Figure 13b shows the finite element modeling of Specimen FBC. In the Specimen FBC, compared to Specimen FB, the EPCW is connected to the columns as well as the beam by high-strength anchor bolts. The anchor bolts were modeled as beam-column elements whose material properties were obtained from mill test results. The anchor bolts were designed to maintain the elastic range at the maximum strength of the walls. In addition, since the wall reinforcement around the anchor bolts was sufficiently strengthened, it was considered that no additional deformation would occur in or around the anchor bolts. In the test, a slip between the column and the wall or deformation in the concrete surrounding the anchor bolts rarely occurred. Table 1 summarizes the cross-sectional areas of each element constituting the walls. The longitudinal elements L1 and L2 were modeled with concrete and reinforcement, while the longitudinal element L3 and the diagonal element D1 were modeled with concrete only, without reinforcement. The cross-sectional area of the longitudinal element was entered as the equivalently split area, while that of the diagonal element was entered as the web width where, through flexural analysis,

tensile stress always occurs under loads in the positive and negative directions. However, in order to accurately consider the shear stress flow in the web, the diagonal element was not modeled in one layer, but divided into two layers, as shown in Figure 11, and the web width of the diagonal element used was 107.3 mm. Figure 13c shows the finite element modeling of Specimen FPB. Like Specimen FB, 12 reinforcement and concrete longitudinal elements were modeled to match the positions of the reinforcements placed on the specimen. Meanwhile, the diagonal element was placed to have an inclination of 55° in terms of the aspect ratio of the specimen, given that the inclination angle of the compression zone is determined according to the size of the actual member. Table 1 shows the cross-sectional areas of each element constituting the walls of Specimen FPB. The longitudinal elements L1 and L2 were modeled with concrete and reinforcement, while the longitudinal element L3 and the diagonal element D1 were modeled with concrete only, without reinforcement, in the same way as Specimen FB. For the cross-sectional area of the diagonal element, 60 mm was applied in consideration of the inclination angle of 55° from the web width of 75 mm where, through flexural analysis, the tensile stress acts, at all times, under loads in the positive and negative directions.

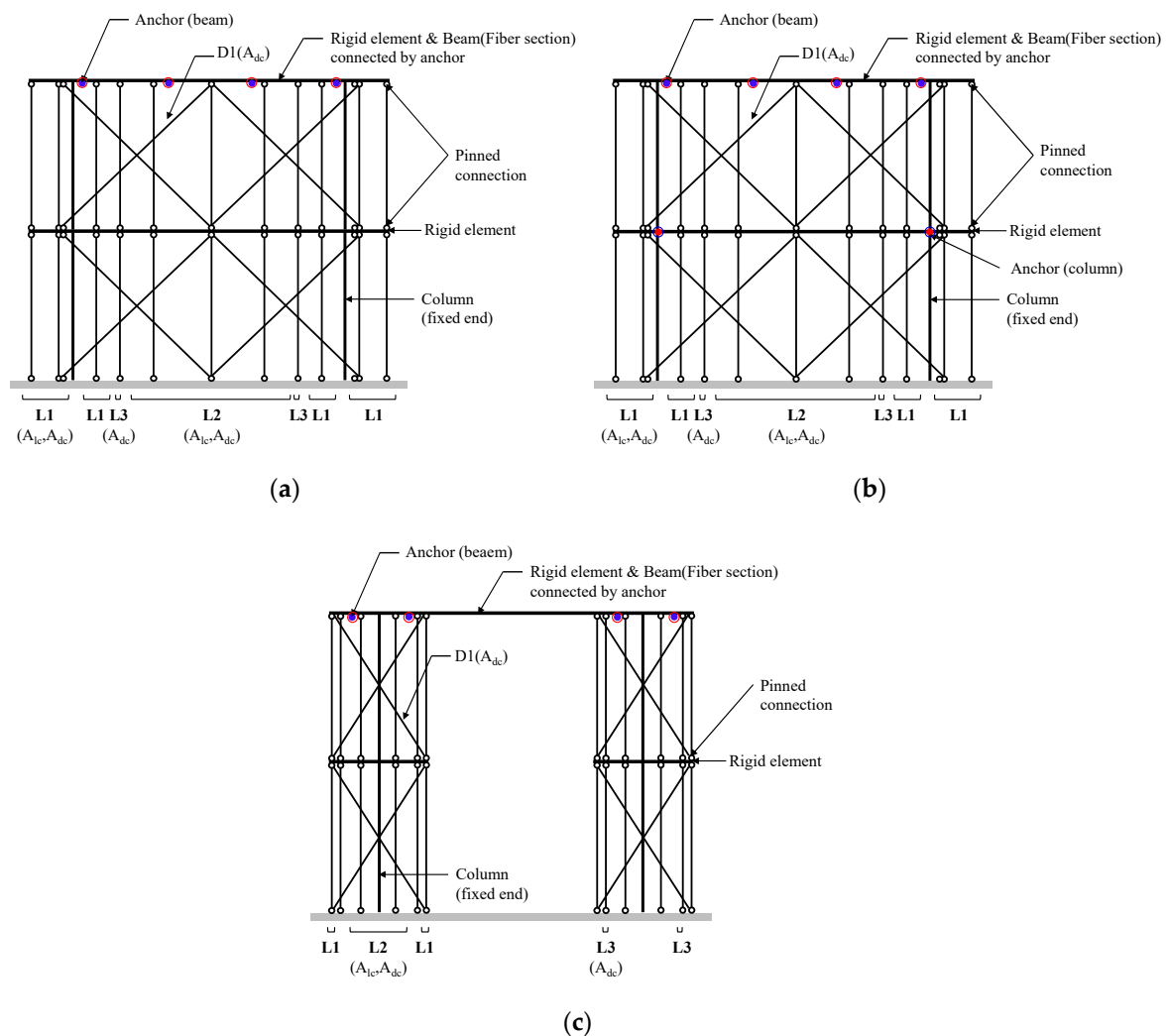


Figure 13. Idealized finite element model of externally anchored precast wall panel (EPCW): (a) Specimen FB; (b) Specimen FBC; (c) Specimen FPB.

Table 1. Cross-section of each element for idealized analysis model.

Cross Section	A _{lc} or A _{dc} (mm ²)	A _{ls} (mm ²)
	Specimen FB, FBC	Specimen FPB
L1	7500	3750
L2	13,125	7500
L3	2812.5	1875
D1	8049.4	4500

5. Verifications of the Analysis Model

5.1. Overall Cyclic Responses and Cumulative Energy Dissipation Capacities

Figure 9 compares the test and analysis results obtained using the modified LDLEM. Table 2 summarizes the maximum strengths in the positive and negative directions in the test and analysis results. The strength ratios of the analysis/test results obtained from Specimen FB were 0.97 and 1.02 in the positive and negative directions, respectively. These strength ratios obtained from Specimen FBC were 0.96 and 0.81 in the positive and negative directions, respectively. These results show that there was a tendency to underestimate the strength of the specimen in the negative direction, but the overall behavior was similar. These strength ratios obtained from Specimen FPB were 1.11 and 1.02 in the positive and negative directions, respectively. Therefore, it was found that the analytical method applied with the modified LDLEM accurately evaluated the overall behavior of specimens strengthened with precast walls.

Table 2. Summary of test and analysis result.

Specimen	Strength(kN)		
	Analysis	Test	Analysis/Test
FB	232.9	238.9	0.97
	-220.6	-216.9	1.02
FBC	229.6	240.1	0.96
	-219.9	-272.1	0.81
FPB	167.4	150.9	1.11
	-161.1	-158.1	1.02
<i>m</i> = 0.98, <i>σ</i> = 0.10			

Figure 14 compares the test and analysis results regarding the secant stiffness of the specimens normalized by the ratio to the initial stiffness. The analysis results were found to accurately evaluate the secant stiffness degradation characteristics, indicating accurate predictions of the strength reduction characteristics according to each loading step.

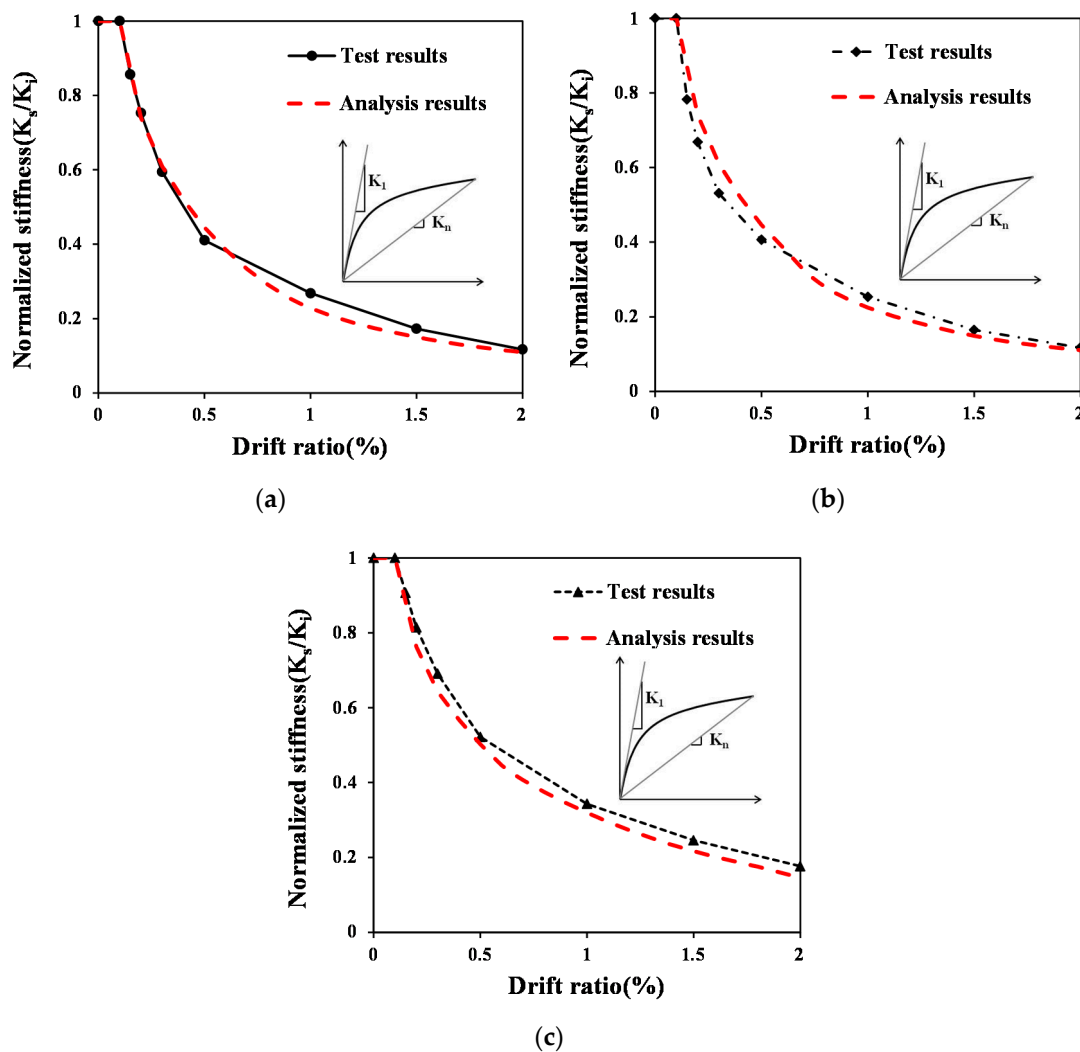


Figure 14. Measured and estimated normalized stiffness: (a) Specimen FB; (b) Specimen FBC; (c) Specimen FPB.

In order for the system to exert sufficient seismic performance, the structure must, after yielding, be able to dissipate sufficient energy. Therefore, cumulative energy dissipation serves as an important indicator related to the seismic performance of structures [4]. Figure 15 compares the amount of cumulative energy dissipation of specimens subjected to cyclic loads, and that of their energy dissipation calculated based on the analysis. In this study, the amount of cumulative energy dissipation was defined as the enclosed area of the load–displacement hysteresis loop. The analysis model provided relatively accurate evaluations of the energy dissipation capacity under cyclic loading. However, the difference between the test and analysis results regarding the energy dissipation capacity of Specimen FBC was relatively larger than that of the other test specimens. This is because a sudden increase in strength occurred in the negative direction during the test of Specimen FBC, as shown in Figure 9b.

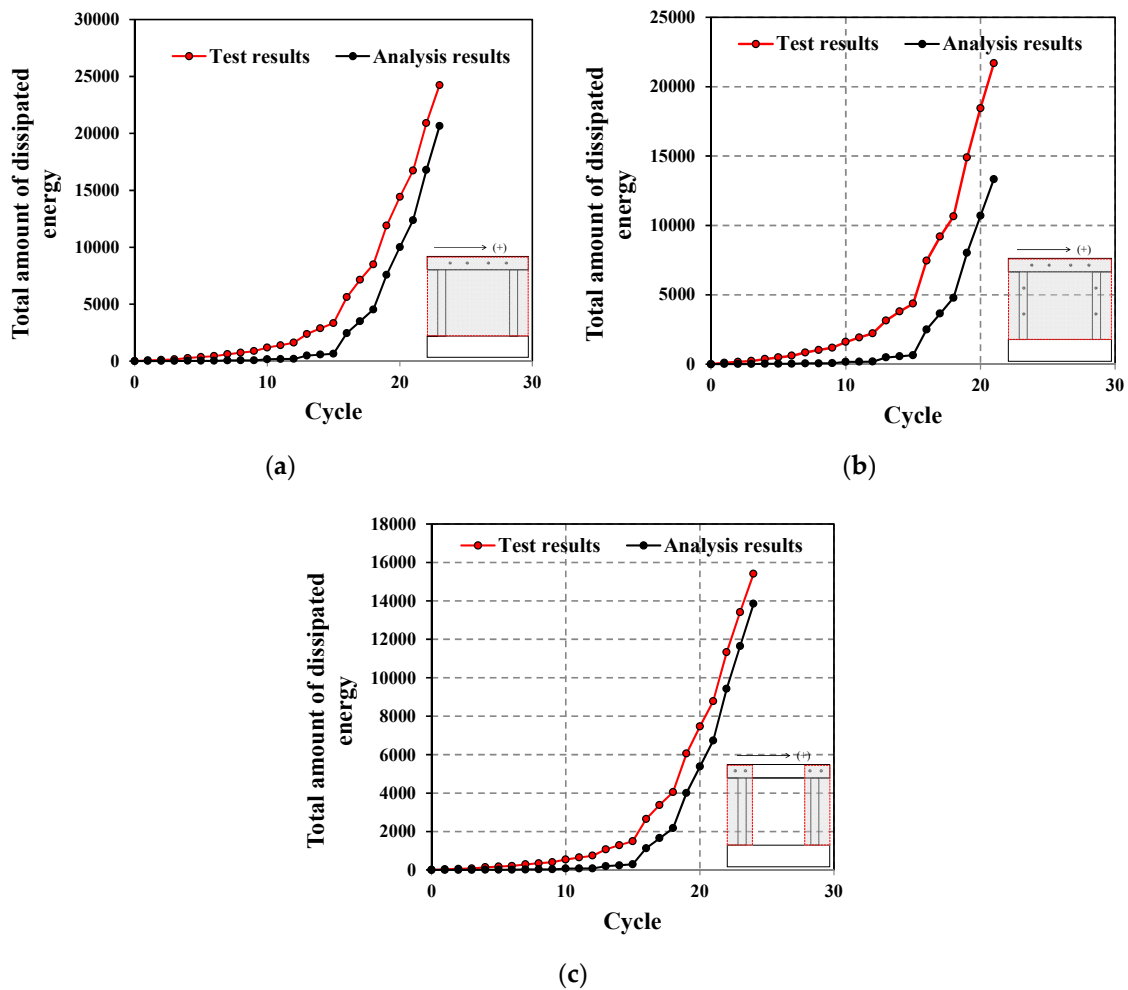


Figure 15. Measured and estimated cumulative energy dissipation: (a) Specimen FB; (b) Specimen FBC; (c) Specimen FPB.

5.2. Failure Mode and Element Behavior

The behavior of the column member was analyzed in detail to verify whether the analytical method presented in this study properly evaluates the failure mode of the specimen. Figure 16 shows the pushover analysis, the moment–curvature relationship and the shear force–shear strain relationship of the column member of Specimen FB. The moment–curvature relationship of the column shown in Figure 16b revealed that the moment of the column increased gradually and, after reaching the flexural strength (M_n), the column exhibited ductile behavior. On the other hand, in the shear force–shear strain relationship of Figure 16c, the shear force did not reach the shear strength (V_n), and the shear strain was recovered with a decrease in shear force at 0.7% drift ratio. The results of Specimens FBC and FPB, shown in Figures 17 and 18, also confirmed that, similar to the characteristics shown in Figure 16, flexure-dominant behavior occurred, and shear was found to behave in the elastic region. These results indicate that, after reaching the flexural strength (M_n), the column exhibits ductile behavior and the precast walls suffer failure. These behavior patterns are consistent with the test results and this leads to the conclusion that the proposed analysis method can adequately predict the failure mode of the columns.

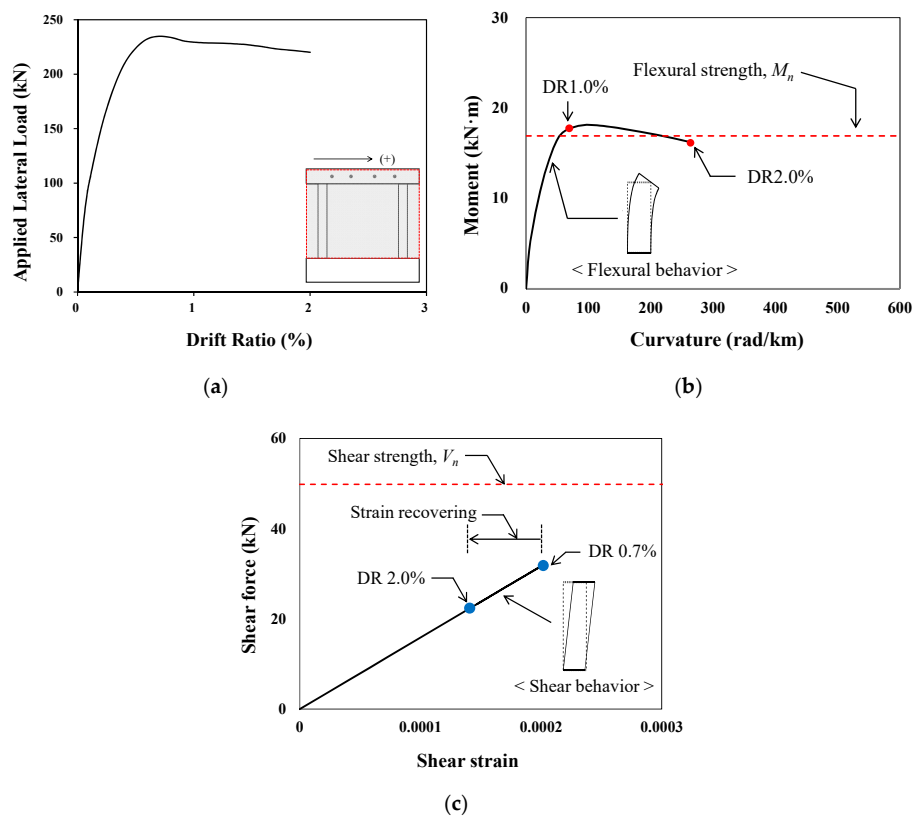


Figure 16. Flexural and shear behavior of column element in Specimen FB: (a) pushover; (b) flexural behavior; (c) shear behavior.

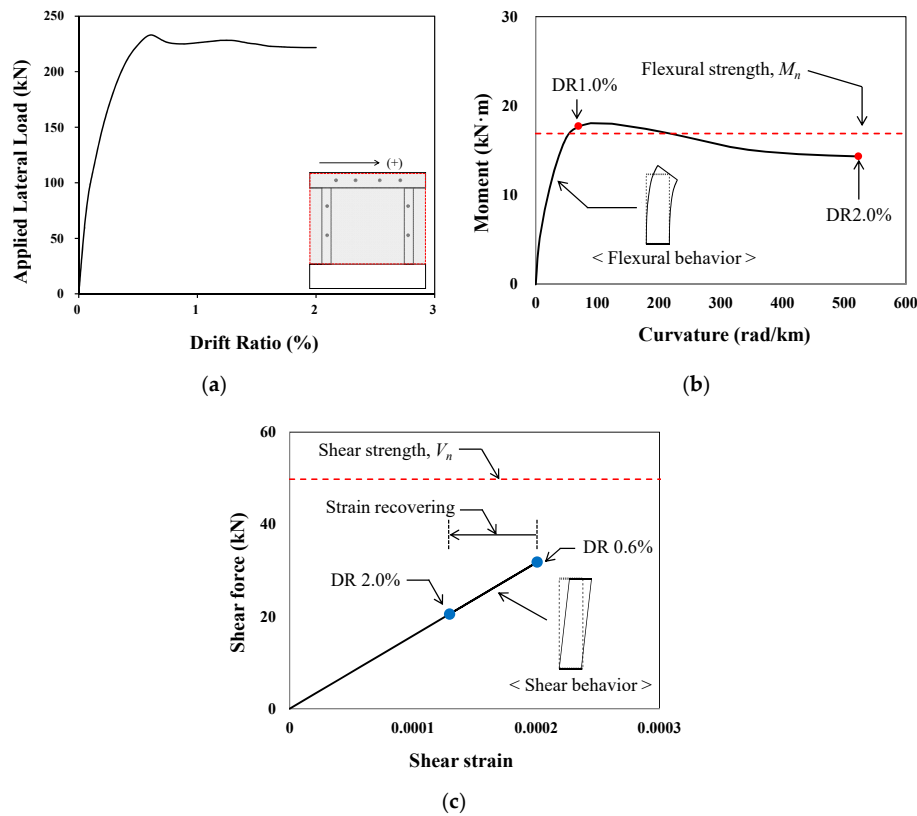


Figure 17. Flexural and shear behavior of column element in Specimen FBC: (a) pushover; (b) flexural behavior; (c) shear behavior.

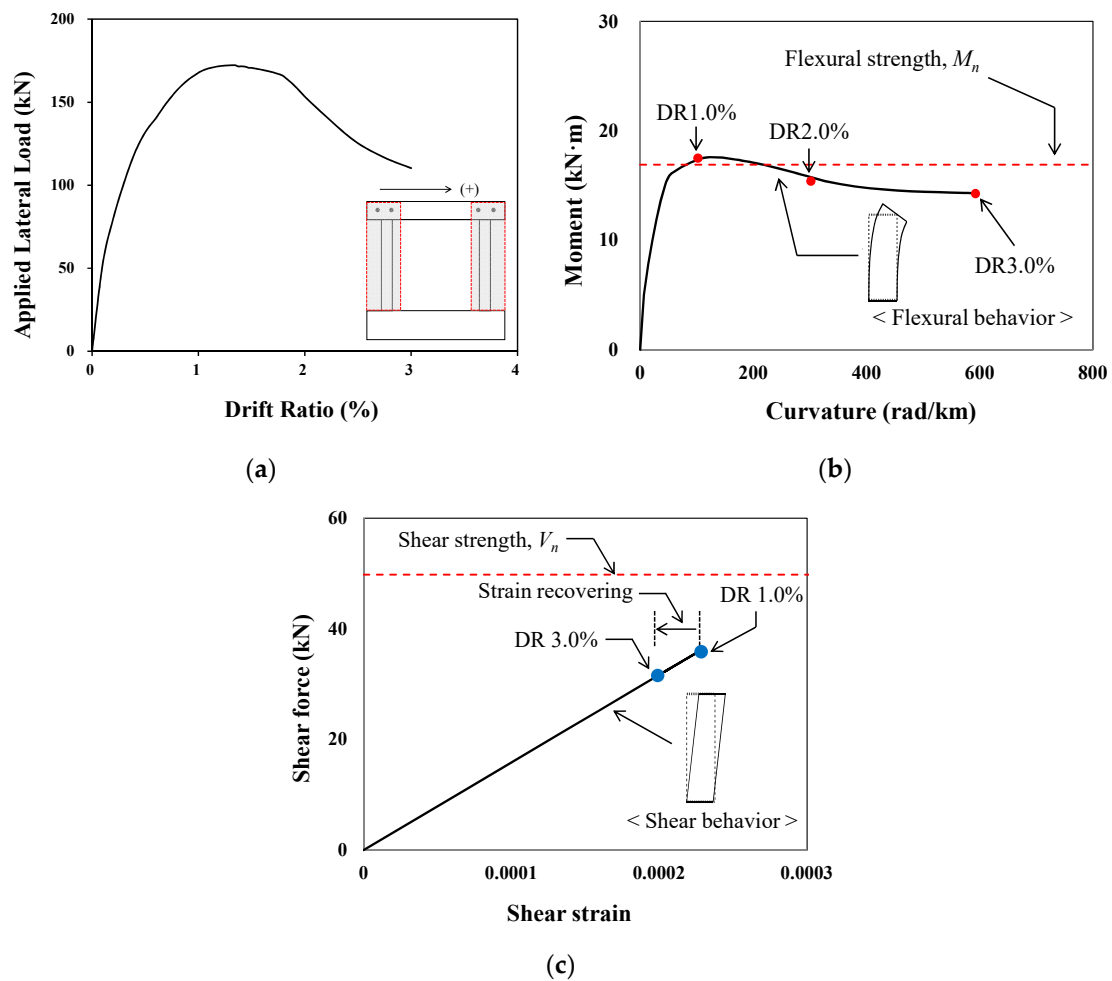


Figure 18. Flexural and shear behavior of column element in Specimen FPB: (a) pushover; (b) flexural behavior; (c) shear behavior.

Figure 9 shows that the overall behaviors of Specimens FB and FBC were similar. However, the curvature analysis results of the columns shown in Figures 16b and 17b demonstrate that, under the same lateral displacement conditions, the curvature was larger in Specimen FBC than in Specimen FB. These results were similar to the test results, in that the column damage was greater in Specimen FBC, in which high-strength anchor bolts were connected to both the beam and column.

At a 2.0% drift ratio, Specimen FPB showed a curvature similar to that of Specimen FB, but when the drift ratio was 2.7%, it showed a similar degree of curvature to that of Specimen FBC. As can be identified from the test results, the column damage was smaller than that of Specimen FBC, thereby helping to achieve superior deformation capacity.

Figures 19–21 show the force–displacement responses of major elements in Specimens FB, FBC and FPB. Since the column of the frame structure shown in Figure 19a was modeled as a nonlinear beam–column element, it was represented by global lateral displacement and global lateral force. On the other hand, the longitudinal and diagonal elements of the wall shown in Figure 19b,c were represented as the axial displacement and axial force, respectively. This was because they were modeled as truss elements. Figure 19a shows that Specimen FB exhibited frame behavior that was similar to that of Specimen FC, and showed a characteristic after the ultimate load in which the load decreased slowly with an increase in displacement. In relation to the longitudinal element of Figure 19b, there was a rapid increase in displacement along with the yielding of reinforcement on the tension side, while elastic behavior occurred on the compression side. Since the diagonal element shown in Figure 19c is a concrete element without reinforcement, it does not resist tension well, but does resist high loads in

compression. In addition, as the strength decreased after reaching the maximum compressive strength, it reached strain softening, unlike the longitudinal element. The force–displacement responses of major elements in Specimen FBC shown in Figure 20 are similar to the results of Specimen FB, as shown in Figure 19. However, it is judged that the local behavior of the column ends results in a difference in some of the deformation capacities. With respect to the longitudinal element of Specimen FPB, as shown in Figure 21b, the strength decreased after reaching the maximum compressive strength, and the maximum tensile strength and the compressive deformation further increased compared to Specimens FB and FBC.

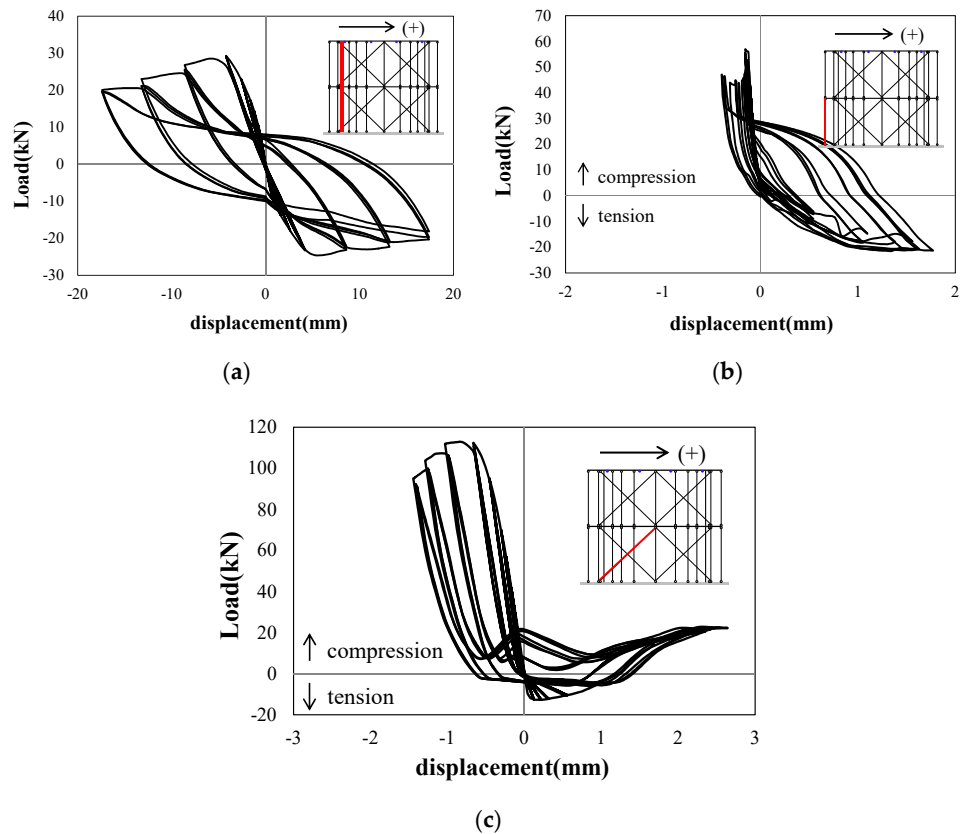


Figure 19. Estimated load–displacement responses of elements in Specimen FB: (a) column; (b) longitudinal element; (c) diagonal element.

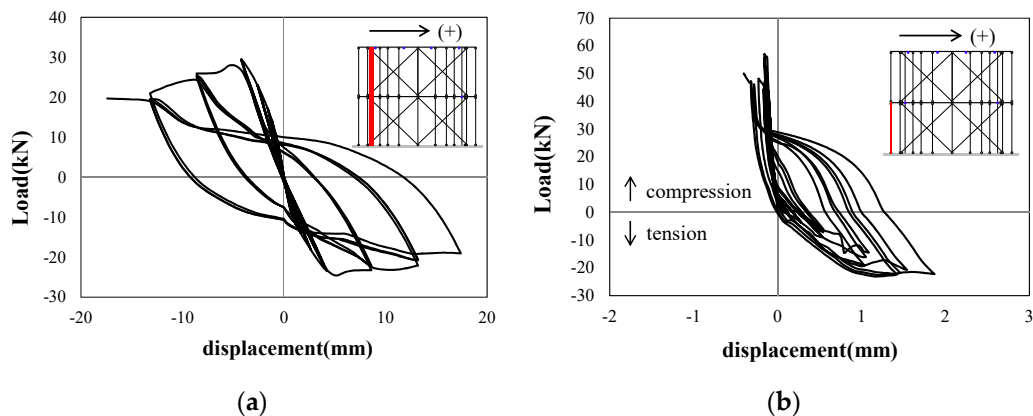


Figure 20. Cont.

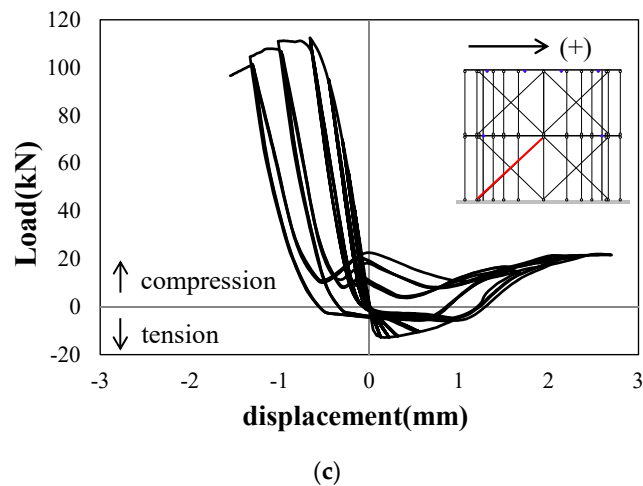


Figure 20. Estimated load–displacement responses of elements in Specimen FBC: (a) column; (b) longitudinal element; (c) diagonal element.

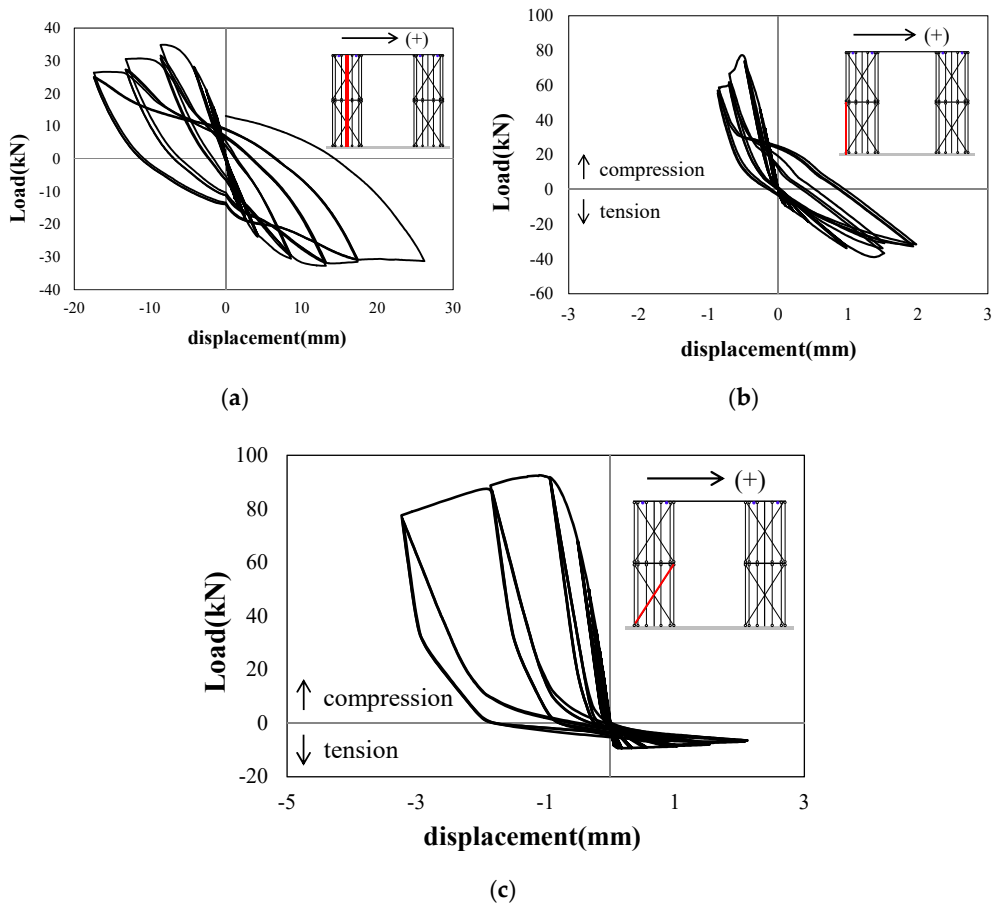


Figure 21. Estimated load–displacement responses of elements in Specimen FPB: (a) column; (b) longitudinal element; (c) diagonal element.

5.3. Simplified Finite Element Model

The analysis model proposed in this study provided relatively accurate predictions of the behavior of frame structures strengthened with precast walls. However, a more simplified analysis model is needed to evaluate the behavior of real size buildings with non-seismic details, as well as buildings strengthened with precast walls.

In a wall, a greater amount of longitudinal reinforcement is generally placed at the end rather than in the center, so as to compose the boundary elements. Using this characteristic, this study proposes a simplified analysis model that reduces the number of longitudinal elements by dividing the walls into both the end and center portions. A total of 11 longitudinal elements, including nine reinforcements and two concrete elements to fill the empty space between the longitudinal reinforcements, were modeled in the idealized analysis model of Specimens FB and FBC, among which three longitudinal reinforcements were included at the end of the wall, with three longitudinal reinforcements and two concrete elements in the center. In the idealized analysis model, the three longitudinal reinforcements at the end of the wall were modeled as three longitudinal elements, while the cross-sectional area of the three longitudinal reinforcements and that of concrete were combined to model one longitudinal element in the simplified analysis model. In the center, three longitudinal reinforcements and two concrete elements were combined to model one longitudinal element, and 11 longitudinal elements were simplified into three elements, as shown Figure 22a,b. In wall modeling, it is an appropriate model decision to design the diagonal element into at least two layers, in order to effectively model shear deformation. Thus, further simplification in the number of elements is no longer available. However, since the vertical element resists axial force and flexural moment, it can be modeled into three elements at both ends and in the center. Figure 22c shows the element model of Specimen FPB, in which the number of longitudinal elements for each wall was reduced to three. Table 3 summarizes the cross-sectional areas of longitudinal elements used in the simplified analysis model, where the cross-section of the diagonal element is the same as that of the idealized model shown in Table 1.

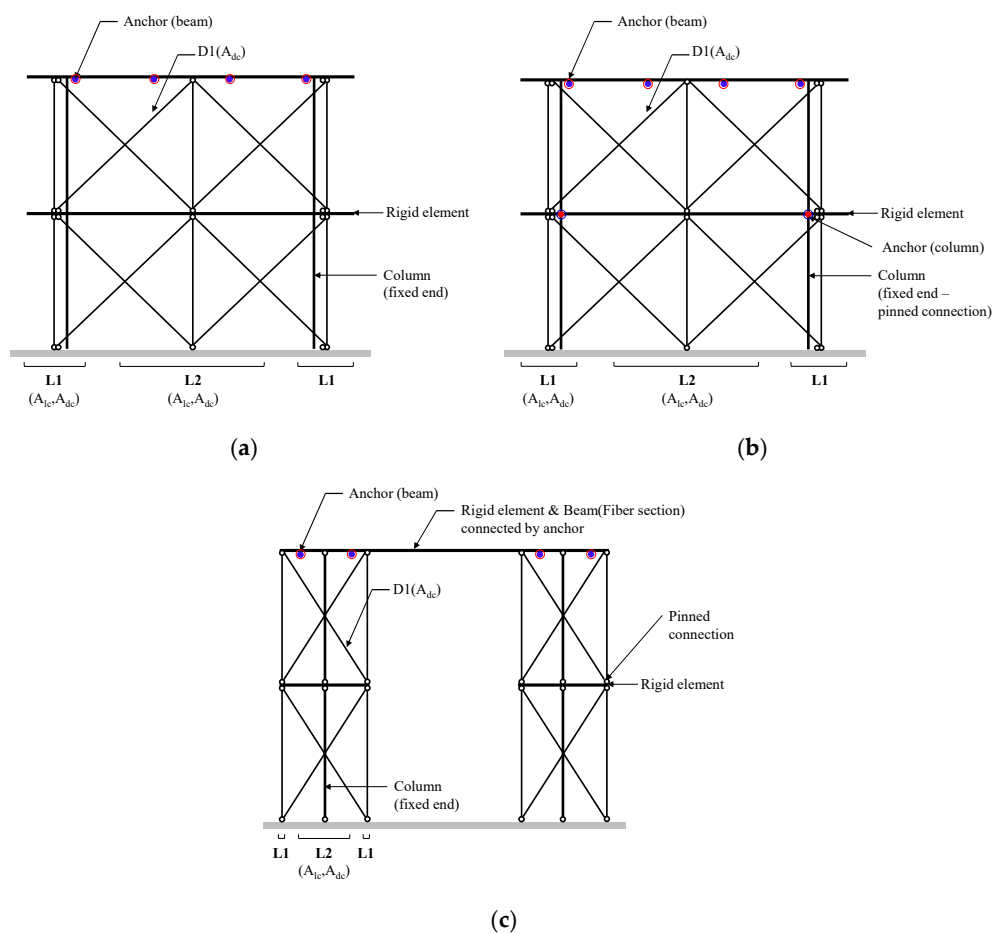


Figure 22. Simplified finite element model of EPCW: (a) Specimen FB; (b) Specimen FBC; (c) Specimen FPB.

Table 3. Cross-section of each element for simplified model.

Cross Section	A_{1c} (mm ²)	A_{1s} (mm ²)
	Specimen FB, FBC	Specimen FPB
L1	22,500	3750
L2	39,375	18,750

Figure 23 shows a comparison between the analysis results of the idealized and the simplified analysis model for each specimen. The analysis results confirmed that the simplified analysis model, which simplified the longitudinal element by dividing the wall into the end and center portions, respectively, showed very similar results to those of the idealized analysis model, which modeled all of the longitudinal reinforcements by dividing them into longitudinal elements. The simplified analysis model is capable of not only shortening the modeling time, but also of reducing the analysis time, by simplifying the longitudinal elements. Therefore, it is expected to facilitate the evaluation of the behavior of a building strengthened with precast walls.

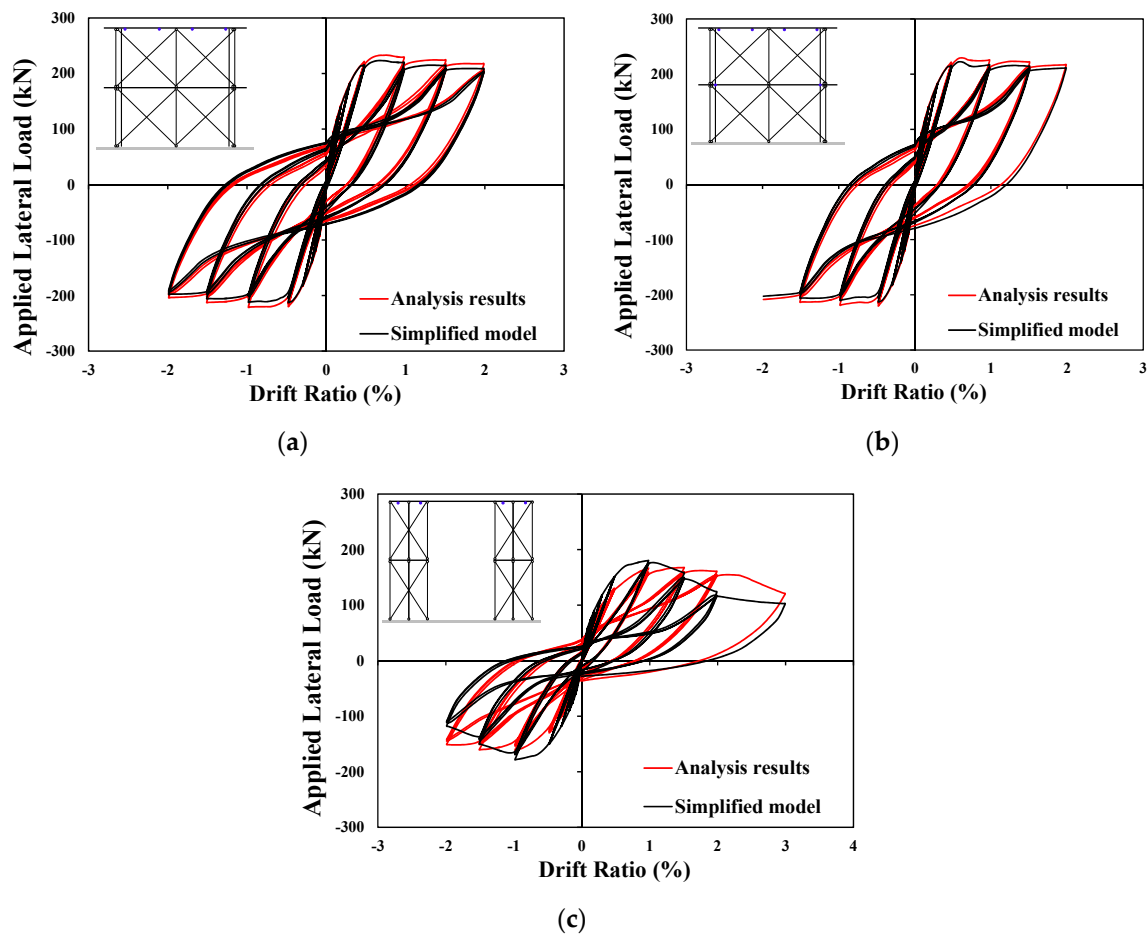


Figure 23. Load–displacement responses of idealized and simplified model: (a) Specimen FB; (b) Specimen FBC; (c) Specimen FPB.

6. Concluding Remarks

In this study, a strengthening method, using an externally anchored precast wall panel (EPCW), was proposed to overcome the disadvantages of the conventional infill wall seismic strengthening method. In order to assess the seismic performance of the proposed model, cyclic loading tests were conducted on the RC frame structures with non-seismic details, and the frame structures were strengthened by

the EPCW method. The nonlinear finite element analysis models using the section aggregator, the fiber section analysis model and the modified LDLEM were also presented, to evaluate the structural behavior of the frame structures strengthened with precast walls. In addition, a simplified analysis model was proposed that was capable not only of reducing the number of longitudinal elements, but also of shortening the modeling and analysis time. The following conclusions can be obtained from this study:

- (1) Specimen FC, an RC frame structure with non-seismic details, exhibited maximum loads of 54.6 and -51.7 kN in the positive and negative directions, respectively. The maximum loads of Specimens FBC and FB (strengthened with EPCW) were 240.1 and 238.9 kN in the positive direction, and -272.1 and -216.9 kN in the negative direction, showing a significant improvement in strength. Specimen FPB, to which the scaled-down EPCW is applied in the form of a wing wall near the column, exhibited maximum loads of 150.9 and -158.1 kN in the positive and negative directions, respectively, showing a great increase in strength. Specimen FPB also exhibited superior deformation capacity, as it showed stable behavior, even at 3.0% drift ratio;
- (2) The modeling of precast walls using LDLEM and section aggregator provided relatively accurate predictions on the overall behavior of the specimens and accurately evaluated the failure mode of the frame structures;
- (3) The test and analysis results confirmed that, compared to Specimen FBC, Specimen FB has relatively superior deformation capacity, and suffers less damage to the column, resulting in more stable lateral behavior. When precast walls are connected to RC frame structures, the connection to the column may lead to large deformation and damage in the column. Therefore, it is advantageous to connect the precast wall only to the beam;
- (4) The simplified analysis model, which simplifies the number of longitudinal elements by dividing the wall into the end and center portions, showed very similar results to the analysis results of the idealized analysis model, which models all of the longitudinal reinforcements into longitudinal elements. Therefore, it is expected that our simplified analysis model can be practically applied to the evaluation of the behavior of buildings;
- (5) It should be noted that the observations drawn from this study are based on the experimental and analytical results of only four specimens; therefore, further study is still required.

Author Contributions: Investigation, H.-E.J. and H.-D.Y.; supervision, K.S.K.; validation, J.-H.H. and S.-J.H.; writing—original draft, S.-H.C.; writing—review & editing, K.S.K. All authors have read and agreed to the published version of the manuscript.

Acknowledgments: This research was funded by the Mid-Career Research Program through the National Research Foundation of Korea (NRF) (NRF-2019R1A2C2086388).

Conflicts of Interest: The authors declare no conflict of interest.

References

1. Frosch, R.J. Seismic Rehabilitation Using Precast Infill Walls. Ph.D. Thesis, Department of Civil Engineering, the University of Texas, Austin, TX, USA, 1996.
2. Frosch, R.J. Panel Connections for Precast Concrete Infill Walls. *ACI Struct. J.* **1999**, *96*, 467–472. [[CrossRef](#)]
3. Almusallam, T.H.; Al-Salloum, Y.A. Behavior of FRP Strengthened Infill Walls under In-Plane Seismic Loading. *J. Compos. Const.* **2007**, *11*, 308–318. [[CrossRef](#)]
4. Ozden, S.; Akguzel, U.; Ozturan, T. Seismic Strengthening of Infilled Reinforced Concrete Frames with Composite Materials. *ACI Struct. J.* **2011**, *108*, 414–422. [[CrossRef](#)]
5. Baran, M.; Tankut, T. Experimental Study on Seismic Strengthening of Reinforced Concrete Frames by Precast Concrete Panels. *ACI Struct. J.* **2011**, *108*, 227–237. [[CrossRef](#)]
6. Koutas, L.; Bousias, S.N.; Triantafillou, T.C. Seismic Strengthening of Masonry-Infilled RC Frames with TRM: Experimental Study. *J. Compos. Const.* **2015**, *19*. [[CrossRef](#)]

7. Harris, H.G.; Ballouz, G.R.; Kopatz, K.W. Preliminary Studies in Seismic Retrofitting of Lightly Reinforced Concrete Frames Using Masonry Infills. In Proceedings of the 6th North American Masonry Conference, Masonry Society (US), Philadelphia, PA, USA, 6–9 June 1993; pp. 383–395.
8. Tomazevic, M.; Zarnic, R. The Behaviour of Horizontally Reinforced Masonry Walls Subjected to Cyclic Lateral in-Plane Reversals. In Proceedings of the 8th European Conference on Earthquake Engineering, Auckland, New Zealand, 30 January–4 February 1984; Volume 4, pp. 1–8.
9. Kabeyasawa, T. US-Japan Cooperative Research on R/C Full-Scale Building Test, Part5: Discussion of Dynamic Response System. In Proceedings of the 8th of WCEE, San Francisco, CA, USA, 21–28 July 1984.
10. Vulcano, A.; Bertero, V. Analytical Model for Predicating the Lateral Response of RC Shear Wall. In *Evaluation of Their Reliability*; EERC, Report No. UCB/EERC-87/19; Earthquake Engineering Research Center, University of California: Berkeley, CA, USA, 1987.
11. Linde, P.; Bachmann, H. Dynamic Modeling and Design of Earthquake-Resistant Walls. *Earthq. Eng. Struct. Dyn.* **1994**, *1331*–1350. [[CrossRef](#)]
12. Milev, J.I. Two Dimensional Analytical Model of Reinforced Concrete Shear Walls. In Proceedings of the 11th of WCEE, Acapulco, Mexico, 23–28 June 1996.
13. Orakcal, K.; Wallace, I.W.; Conte, J.P. Flexural Modeling of Reinforced Concrete Walls-Model Attribute. *ACI Struct. J.* **2004**, *101*, 688–698. [[CrossRef](#)]
14. Park, H.G.; Eom, T.S. Truss Model for Nonlinear Analysis of RC Members Subject to Cyclic Loading. *J. Struct. Eng.* **2007**, *133*, 1351–1363. [[CrossRef](#)]
15. Taucer, F.F.; Spacone, E.; Filippou, F.C. *A Fiber Beam-Column Element for Seismic Response Analysis of Reinforced Concrete Structures*; Report No. UCB/EERC-91/17; Earthquake Engineering Research Center, University of California: Berkeley, CA, USA, 1991; pp. 1–138.
16. Spacone, E.; Ciampi, V.; Filippou, F.C. *A Beam Element for Seismic Damage Analysis*; Report No. UCB/EERC-92/07; Earthquake Engineering Research Center, University of California: Berkeley, CA, USA, 1992; pp. 1–111.
17. Neuenhofer, A.; Filippou, F.C. Evaluation of Nonlinear Frame Finite-Element Models. *J. Struct. Eng.* **1997**, *123*, 958–966. [[CrossRef](#)]
18. Neuenhofer, A.; Filippou, F.C. Geometrically Nonlinear Flexibility-Based Frame Finite Element. *J. Struct. Eng.* **1998**, *124*, 704–711. [[CrossRef](#)]
19. Kim, D.K.; Eom, T.S.; Lim, Y.J.; Lee, H.S.; Park, H.G. Macro Model for Nonlinear Analysis of Reinforced Concrete Walls. *J. Korea Concr. Inst.* **2011**, *23*, 569–579. [[CrossRef](#)]
20. Otani, S. *A Computer Program for Inelastic Analysis of R/C Frames to Earthquake*; A Report on Research Project No.413; University of Illinois Urbana: Champaign, IL, USA, 1974; pp. 1–8.
21. OpenSees. *Open System for Earthquake Engineering Simulation, Pacific Earthquake Engineering Research Center*; University of California: Berkeley, CA, USA, 2004; pp. 1–465.
22. Vecchio, F.J.; Collins, M.P. The Modified Compression-Field Theory for Reinforced Concrete Elements Subjected to Shear. *ACI Struct. J.* **1986**, *83*, 219–231. [[CrossRef](#)]
23. Bentz, E.C.; Vecchio, F.J.; Collins, M.P. Simplified Modified Compression Field Theory for Calculating Shear Strength of Reinforced Concrete Elements. *ACI Struct. J.* **2006**, *103*, 614–624. [[CrossRef](#)]
24. Yassin, M.H.M. Nonlinear Analysis of Prestressed Concrete Structures under Monotonic and Cycling Loads. Ph.D. Thesis, University of California, Berkeley, CA, USA, 1994.
25. Mander, J.B.; Priestley, M.J.N.; Park, R. Theoretical Stress-Strain Model for Confined Concrete. *J. Struct. Eng.* **1988**, *114*, 1804–1826. [[CrossRef](#)]
26. Filippou, F.C.; Popov, E.P.; Bertero, V.V. *Effects of Bond Deterioration on Hysteretic Behavior of Reinforced Concrete Joints*; Report EERC 83-19; Earthquake Engineering Research Center, University of California: Berkeley, CA, USA, 1983.
27. Laura, N.L.; Nilanjan, M.; Arash, A. *A Beam-Column Joint Model for Simulating the Earthquake Response of Reinforced Concrete Frames*; PEER Report; Pacific Earthquake Engineering Research Center, College of Engineering University of California: Berkeley, CA, USA, 2004.

